Scientific Reports

https://doi.org/10.1038/s41598-026-39347-0

Article in Press

Separation of large droplets from an oil-in-water emulsion using a deterministic lateral displacement (DLD) microfluidic chip

Received: 18 November 2025

Accepted: 4 February 2026

Published online: 20 February 2026

Cite this article as: Hong H., Lee E., Hwangbo S. *et al.* Separation of large droplets from an oil-in-water emulsion using a deterministic lateral displacement (DLD) microfluidic chip. *Sci Rep* (2026). https://doi.org/10.1038/s41598-026-39347-0

Hyeonji Hong, Eunbi Lee, Seonae Hwangbo & Il Doh

Separation of Large Droplets from an Oil-in-Water Emulsion using a Deterministic Lateral Displacement (DLD) Microfluidic Chip

Hyeonji Hong[a, †], Eunbi Lee[b, †], Seonae Hwangbo[b], and Il Doh[a, c, *]

[a] Medical Metrology Group, Division of Biomedical Metrology, Korea Research Institute of Standards and Science (KRISS), Republic of Korea

[b] Focused Ultra-Sonic Technology Lab (FUST LAB), Daejeon 34015, Republic of Korea

[c] Department of Applied Measurement Engineering, University of Science and Technology (UST), Republic of Korea

[†]Both authors are contributed equally.

[*]Corresponding author:

Il Doh

E-mail: il.doh@kriss.re.kr

Tel: +82-42-868-5589

Fax: +82-42-868-5455

ABSTRACT

Long-term stability of oil-in-water (O/W) emulsions is often compromised by the presence of larger droplets, which act as seeds for coalescence and phase separation. Conventional separation methods like filtration and centrifugation face challenges such as high energy consumption and filter clogging. In this study, we present a deterministic lateral displacement (DLD) microfluidic chip for the continuous and passive separation of larger oil droplets to enhance emulsion homogeneity and stability. A PDMS-based DLD chip, featuring a micropillar array with a pillar diameter of 20 µm and a gap of 5 µm, was designed to achieve a theoretical critical separation diameter (D_c) of approximately 1.7 µm. The separation mechanism was validated using a numerical estimation and experiments with fluorescent polystyrene beads. We successfully demonstrated that the DLD chip effectively removes larger droplets from ultrasonically prepared nanoemulsions, reducing the median particle diameter (D_{50}) from 1.103 µm to 0.768 µm without using any surfactants. The results confirm that the DLD-based post-processing is a promising method for improving the quality of O/W emulsions, although challenges related to the fabrication of high-aspect-ratio structures and the pressure tolerance of PDMS must be addressed for high-throughput applications.

Keywords: Deterministic Lateral Displacement (DLD), Microfluidics, Oil-in-Water Emulsion, Droplet Separation, Droplet Microfluidics

1. Introduction

Oil-in-water (O/W) emulsions, where oil droplets are stably dispersed within a continuous aqueous phase, are widely utilized across various industries due to their unique ability to combine hydrophobic and hydrophilic components [1]. In cosmetics, O/W emulsions play a crucial role in improving product texture, stability, and enhancing delivery of active ingredients to the skin [2]. In the pharmaceutical field, O/W emulsions are employed as effective delivery vehicles for Active Pharmaceutical Ingredients (APIs), enhancing bioavailability [3]. The food industry also relies on them to achieve desired textures and product stability [4]. The effectiveness of O/W emulsions in all these applications critically depends on their stability and physical properties, which demand advanced technology for high-quality emulsion production and control.

Traditional approaches to emulsion preparation include high-pressure homogenization [5], ultrasound-assisted emulsification,[6] and microfluidic systems [7–9]. The emulsions produced by these methods, however, often exhibit instability over time due to phenomena such as coalescence, creaming, and flocculation [10], which can lead to phase separation. Larger droplets, even in trace amounts, can serve as nucleation sites for coalescence due to their lower surface energy and larger collision cross-section relative to smaller droplets. Therefore, the instability can be mitigated by eliminating larger droplets and reducing droplet size below a critical threshold, as Brownian motion becomes more dominant than gravity-driven particle migration under these conditions [11,12]. Consequently, minimizing droplet size and achieving a narrow size distribution during the manufacturing process are essential for enhancing emulsion stability. In particular, emulsions composed solely of oil droplets in the absence of surfactants lack interfacial stabilization, thereby

necessitating the reduction of droplet size to the sub-micron scale to ensure kinetic stability.

Conventional techniques for selective removal of large particles in emulsions, such as membrane filtering,[13,14] centrifugation,[15], suffer from significant limitations in process efficiency, including high energy consumption, filter clogging, and unsuitability for large-scale, continuous operations. With recent advancements in microfluidics, research into the precise manipulation and separation of droplets or particles within microscale channels has become active [16,17]. While microfluidic-based particle separation technologies offer advantages like precision, miniaturization, and continuous processing, their practical application has been constrained by challenges in separating sub-micron particles and by low throughput, which limits their use in mass production.

Deterministic Lateral Displacement (DLD) is a prominent passive microfluidic separation method that utilizes the principle of path differentiation based on the size of droplets or particles flowing through a periodic array of microstructures [18]. Particles larger than a specific critical diameter (D_c) are continuously displaced laterally by interacting with the pillars and are separated into a designated path. In contrast, smaller particles follow the fluid streamlines, allowing for the effective and continuous separation of particles above and below the critical size. Previous studies have demonstrated high-efficiency separation of satellite droplets from main droplets population in an emulsion [19], and have explored separation possibilities based on droplet viscosity and deformation characteristics [20–22]. While most reported DLD research has concentrated on micron-scale particles and droplets, its application to nm-range separation has been restricted to small quantities and low-flow-rate conditions [23–25].

In this study, we aimed to enhance the uniformity and stability of an O/W emulsion by effectively separating potentially destabilizing large oil droplets using a DLD-based microfluidic chip. As illustrated in **Figure 1**, after an emulsion is prepared by an ultrasonic emulsification system, a DLD microfluidic chip serves as a post-processing step to selectively separate particles larger than a specific size. Compared to the unprocessed sample (1), the separated sample (2) is expected to have a smaller average particle size and improved emulsion stability.

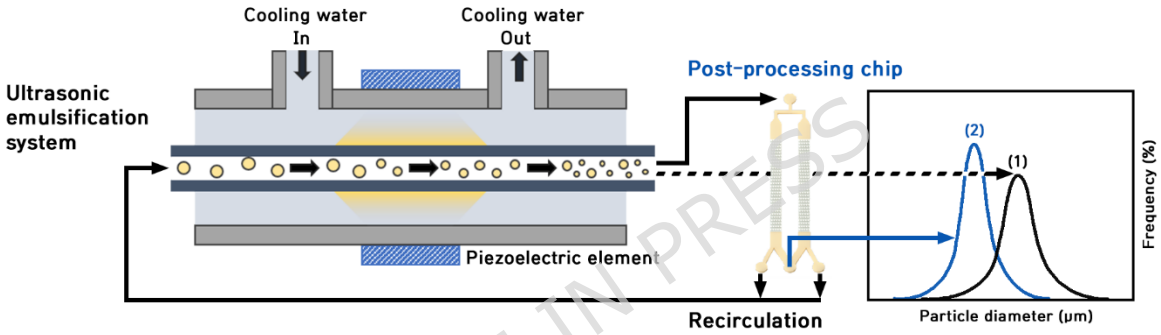

Figure 1 Schematic of the ultrasonic emulsification system and the particle size distributions for a sample (1) before and (2) after post-processing chip.

2. Materials and methods

2.1. Deterministic Lateral Displacement (DLD)

Deterministic Lateral Displacement (DLD) is a microfluidic separation technique based on the principle that particles of different sizes follow distinct paths as they pass through a fluid flowing around a regularly arranged array of micropillars. A typical DLD device contains a periodic array of pillars within a fluidic channel, with each row of pillars shifted by a small angle relative to the direction of flow. The fluid forms distinct streamlines as it passes between the pillars, and particles either

follow these streamlines or are deflected depending on their size.

The core concept of DLD is defined by the critical diameter (D_c). As shown in **Figure 2a**, particles with a diameter smaller than D_c follow the fluid streamlines in a "zigzag mode," experiencing no net lateral displacement. Conversely, particles larger than D_c are consistently bumped laterally by the pillar array, following a "displacement mode". Thus, a DLD device can induce two completely different trajectories based on particle size under a single flow condition, enabling the selective removal of particles larger than a specific size.

The critical diameter is determined by the geometric parameters of the pillar array, specifically the gap between pillars (G) and the row shift fraction (ε). An empirical formula to approximate D_c is given by

$$D_c \approx 1.4G\varepsilon^{0.48} \quad (1)$$

In Eq. (1), ε is the row shift fraction, defined as the ratio of the lateral shift of a row (σ) to the center-to-center pillar distance (λ), which can also be expressed as $\varepsilon = tan\theta$ [26]. By designing the pillar array geometry, a specific D_c can be set to selectively separate particles. A key advantage of DLD is that separation is based on the physical property (size) of the particles, enabling continuous and precise separation without external fields or complex equipment. Unlike conventional membrane filtration or centrifugation, this method is non-contact and non-destructive, and it maintains stable separation performance under constant flow conditions.

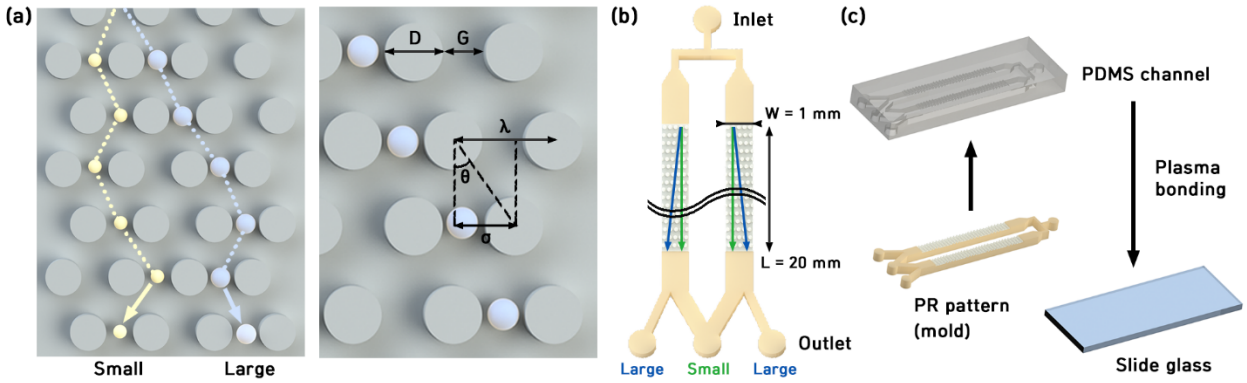

Figure 2 Deterministic Lateral Displacement (DLD) chip: (a) Principle of Deterministic Lateral Displacement (DLD), showing smaller particles in zigzag mode and larger particles in displacement mode. Key geometric parameters are defined. (b) Schematic of the designed chip with two parallel channels (W = 1 mm, L = 20 mm). (c) The fabrication process of the PDMS-based DLD device using soft lithography.

For the main device used in our experiments, the pillar array geometry was as follows: pillar diameter D = 20 μm, gap G = 5 μm, and center-to-center distance λ = 25 μm. The array was designed with a displacement angle of θ = 3°, resulting in a row shift distance of $\sigma \approx 1.31$ μm. Based on these parameters, the theoretical critical diameter D_c is calculated to be approximately 1.7 μm. **Figure 2b** shows a schematic of the experimental chip. To increase throughput, two symmetric channels were connected in parallel, featuring one inlet and three outlets. The pillar arrays were oriented to direct large particles towards the outer side walls, which lead to two separate outlets, while smaller particles were collected from the central outlet. The width (W) of each channel was set to 1 mm, and the length (L) was set to approximately 20 mm to ensure that particles larger than D_c could fully migrate across the channel width for effective separation.

Based on the size of the channel, when water is injected at a flow rate of 1 mL/h, the Reynolds number ($Re = D_h U\rho/\mu$) calculated for the flow is 0.03, confirming that the flow is laminar. In this case, D_h is the hydraulic diameter, U is the fluid velocity, and ρ and μ are the density and viscosity of water, respectively. At such low Reynolds numbers, inertial effects are negligible, and the separation mechanism is primarily driven by factors such as viscous forces. Thus, two or more fluids flow in parallel without mixing, except for diffusion, and then different trajectories based on particle size can be explained according to the DLD channel structure [26].

2.2. Numerical Estimation

The flow characteristics inside the DLD microfluidic chip were predicted using the commercial finite element software COMSOL Multiphysics (COMSOL Inc., Sweden). The simulation was performed to visualize the flow field and streamline patterns generated by the pillar array and to confirm the size-dependent particle trajectory differences. The geometric model for the simulation was identical to the fabricated DLD chip. The pillar diameter and array periodicity were set to match the experimental conditions, and the analysis was conducted using a 3D laminar flow module. The fluid was assumed to be an incompressible Newtonian fluid operating under steady-state laminar flow conditions. The flow field was governed by the continuity equation and the steady-state Navier-Stokes equation as in Eqs. (2) and (3).

$$\nabla \cdot \boldsymbol{u} = 0 \tag{2}$$

$$\rho(\boldsymbol{u} \cdot \nabla)\boldsymbol{u} = -\nabla p + \mu \nabla^2 \boldsymbol{u} \tag{3}$$

where ρ is the fluid density, $\boldsymbol{u}$ is the velocity vector, p is the pressure, and μ is the dynamic viscosity. A normal inflow velocity condition was set, corresponding to the

experimental flow rates and outlet pressure boundary condition was set to zero ($p = 0$) at the exit ports. A no-slip condition applied to all pillar surface and channel walls to account for the viscous effects.

The simulation results, shown in **Figure 3a**, indicate that high-velocity regions form between the pillars in each row along the flow direction (y-axis) [27]. The periodic redistribution of the fluid by the pillar array creates the characteristic zigzag streamlines. As shown in the inset of **Figure 3a**, the streamlines are compressed and shifted laterally as they navigate the gaps between pillars. The first streamline closest to the pillar surface is deflected and follows the pillar row shift, leading to the lateral displacement of particles larger than D_c [28,29]. Smaller particles, however, can remain within the initial set of streamlines and thus follow a zigzag path with no net displacement as in **Figure 3b**. These simulation results support the theoretical concept of the critical diameter and predict the differential migration modes based on particle size for our designed pillar array.

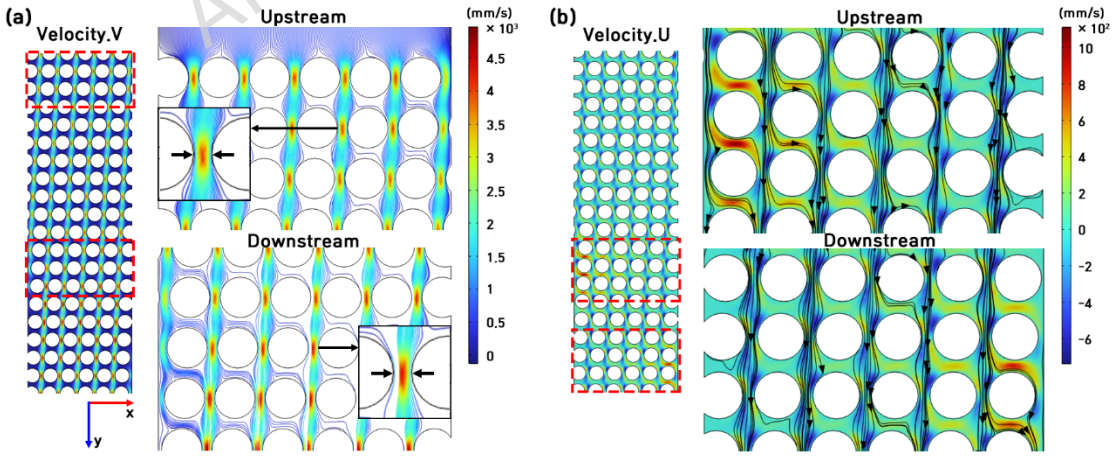

Figure 3 Numerical simulation of flow in the DLD channel: velocity contours and streamlines for the (a) primary flow direction (y-axis) and (b) lateral direction (x-axis).

2.3. Microfluidic Device Fabrication

The DLD microfluidic chip used in this study was fabricated using a standard Polydimethylsiloxane (PDMS) and soft lithography method (**Figure 2c**). First, a master mold was created by spin-coating SU-8 photoresist (SU-8 2050, MicroChem) onto a silicon wafer to form a light-sensitive layer of the desired thickness. The DLD structure was then patterned onto the resist using photolithography with a photomask, followed by development to create the final pillar array mold.

A mixture of PDMS prepolymer (Sylgard 184, Dow Corning) and a curing agent (10:1 ratio by weight) was poured over the master mold and degassed in a vacuum chamber to remove air bubbles. The PDMS was cured in an oven at 70 °C for approximately 2 hours and then carefully peeled from the master mold. **Figure 4a** shows the fabricated PDMS chip bonded to a glass slide and the experimental setup. A syringe pump injects the sample into the inlet, and separated fractions are collected from the three outlets. For analysis, samples of smaller, filtered particles were collected from the central outlet. **Figure 4b** displays top-down and cross-sectional views of the PDMS pillar array. The pillars showed a relatively uniform diameter from the bottom to the top of the channel. Inlet and outlet ports were created using a 1-mm biopsy punch. Finally, the PDMS chip and a glass slide were treated with oxygen plasma (50 W, 30 s) to activate their surfaces for irreversible bonding. The completed microfluidic device was then connected to a flow control system for experiments.

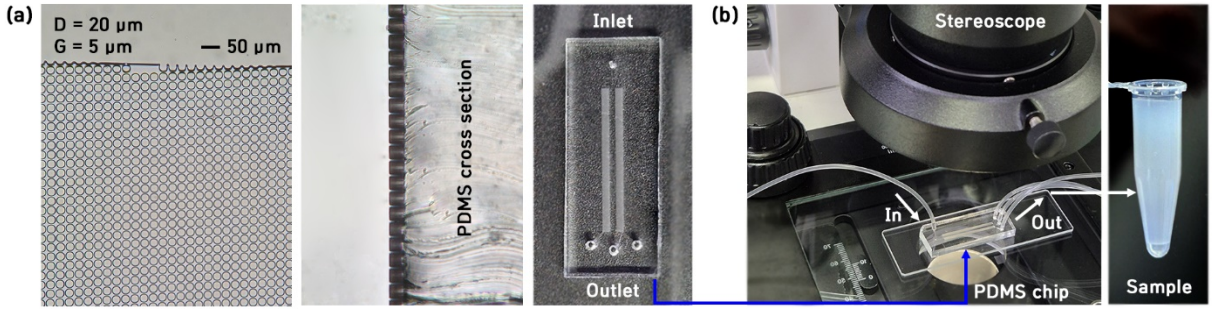

Figure 4 Fabricated microfluidic chip and experimental setup: (a) A PDMS chip and enlarged image of micropillar array with a magnified top-down view of the micropillar array and a cross-sectional image showing the profile of the pillars (b) The experimental setup showing the fabricated PDMS chip mounted on a stereoscope for observation. The sample is injected via the inlet ("In") and collected from the outlets ("Out").

2.4. Nanoemulsion Preparation

The nanoemulsion was prepared using a cylindrical focusing ultrasonic device (DEBREX; Fust Lab Co., Ltd., Daejeon, Korea) equipped with a lead zirconate titanate (PZT) transducer. This device focuses ultrasonic energy at the center of the sample, inducing intense cavitation and shear forces, which provides more uniform dispersion compared to other ultrasonic devices. For this study, a PZT operating at a frequency of 380 kHz and a fixed power of 100 W was used. The aqueous phase was injected at a flow rate of 20–30 mL/min, while the oil phase was simultaneously injected at a constant rate of 0.5 mL/min through a dual inlet. The total processing time was adjusted to achieve the target mean particle size. The high-energy cavitation inside the chamber rapidly dispersed the oil droplets, forming a uniform nanoemulsion. For this experiment, an emulsion with a mean particle size distribution of approximately 1 µm was prepared to evaluate the chip's effectiveness in separating micron-sized particles. The freshly prepared emulsion was immediately used in the microfluidic separation process.

2.5. Experimental Setup

Two types of experiments were conducted to verify the separation performance of the fabricated DLD microfluidic chip. First, to visualize the size-dependent separation mechanism, fluorescent polystyrene beads with diameters of 1 μm and 2 μm (Thermo Fisher Scientific, United States) were used. The bead suspension was injected into the chip at a constant flow rate (0.5–2 μL/min) using a syringe pump (Legato 210, KD Scientific Inc., United States), and the particle trajectories were observed in real-time with a fluorescence microscope (Axio Scope A.1, Zeiss Microscopy, Germany). For the actual O/W emulsion separation experiments, the process was monitored using a high-speed camera (Phantom VEO 310L, Vision Research, United States). The trajectories of the oil droplets flowing inside the chip were recorded at a frame rate of 2,000 fps.

2.6. Nanoemulsion Size Analysis

The particle size distribution of the emulsion samples before and after separation by the DLD chip was measured using a laser diffraction particle size analyzer (LA-960, Horiba Ltd., Kyoto, Japan). The analysis was performed in wet circulation mode, with a magnetic stirrer ensuring the sample remained uniformly dispersed. The instrument calculates particle size and distribution by analyzing the angular distribution of scattered light when a laser beam illuminates the sample. Samples were diluted with deionized (DI) water to achieve a light transmission value in the range of 83–89% before measurement. The results were presented as the median particle diameter (D_{50}) and cumulative distribution values (D10, D90) to evaluate the change in size distribution before and after separation.

3. Results and Discussion

3.1. Particle Trajectory

Preliminary tests were conducted using an oil emulsion and the fabricated PDMS DLD chip to confirm whether oil droplets separate by size as predicted by the simulations. The initial sample had a mean particle size of 2.5 μm with a distribution ranging from 1.4 to 3.7 μm. The DLD array used had a calculated D_c of approximately 1.8 μm. **Figure 5a** shows time-lapsed images (24 fps) of the sample flowing through the DLD channel at 1 mL/h.

Over time, the larger, microscopically observable particles were deflected toward one side of the channel, concentrating near the channel wall after 5 seconds of flow. **Figure 5b** shows the separation of an oil sample in a DLD array with a pillar diameter of 20 μm and a gap of 5 μm (D_c = 1.7 μm). The pillar aspect ratio was slightly modified to enhance the structural stability of the PDMS pillars during fabrication and bonding. The emulsion used here had a mean particle size of 1.1 μm (ranging from 669 nm to 1.59 μm), and again, larger particles were observed to be deflected to one side for separation. To investigate the possibility of droplet deformation, Capillary number (Ca) was calculated by using the following equation.

$$Ca = \mu U/\gamma \quad (4)$$

, where μ is the viscosity of the continuous phase, U is the characteristic flow velocity, and γ is the interfacial tension. The viscosity of water and the interfacial tension between water and oil are set to μ = 1 mPa□s and γ = 23 mN/m respectively, and the flow rate conditions used in the experiment are set to 1 mL/h. At sufficiently low Ca, interfacial tension dominates over viscous stress, and droplets retain a near-spherical shape, behaving similarly to rigid particles. Under our operating

conditions, the estimated value is 6.04×10^{-6}, remaining in a low-*Ca* regime (*Ca* << 1). Consequently, the oil droplets maintain an effective hydrodynamic diameter, and mode transition from zigzag to displacement (or vice versa) is suppressed.

After confirming the chip's ability to displace oil droplets larger than D_c, we used particles of a known size to clearly differentiate the flow behavior. **Figure 6a** shows fluorescent images of 1-μm and 2-μm particles flowing through the same channel, captured at the same position (approximately 3/4 down the channel length). While the 1-μm particles are distributed across a wide area of the channel, the 2-μm particles are clearly deflected toward the channel wall, flowing in a narrow stream. **Figure 6b** compares the flow of 0.5-μm particles alone with a mixed sample of 0.5-μm and 2-μm particles. The 0.5-μm particles are distributed evenly toward both sides of the central outlet, whereas the 2-μm particles are displaced and exit through only one side of the outlet path. **Figure 6c** shows the trajectory of 2-μm particles at different positions along the channel. As the particles flow from upstream to downstream, they become increasingly concentrated, forming a thicker and brighter line near the wall. These observations are consistent with the expected separation behavior for our DLD array design, which was intended to separate particles larger than the calculated D_c of 1.7 μm.

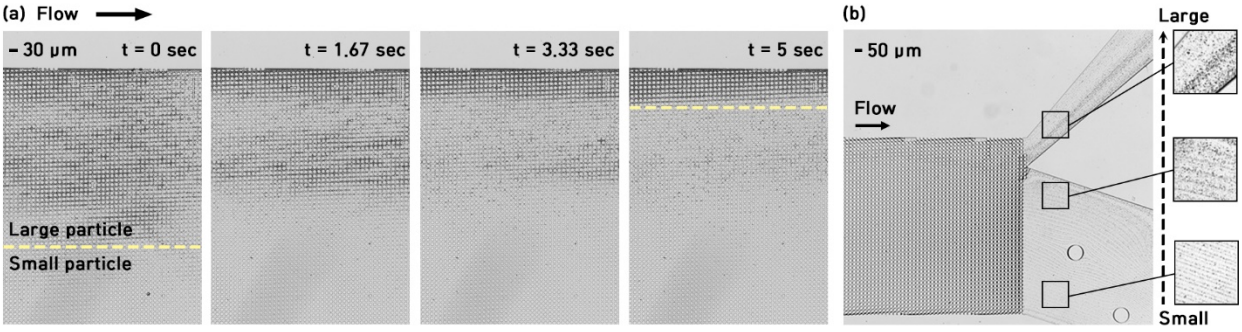

Figure 5 Droplet separation inside the DLD array: (a) Time-lapsed images showing the

lateral migration of larger oil droplets as they flow through the micropillar array, (b) Separation of oil droplets at the outlet of a DLD channel with modified pillar geometry.

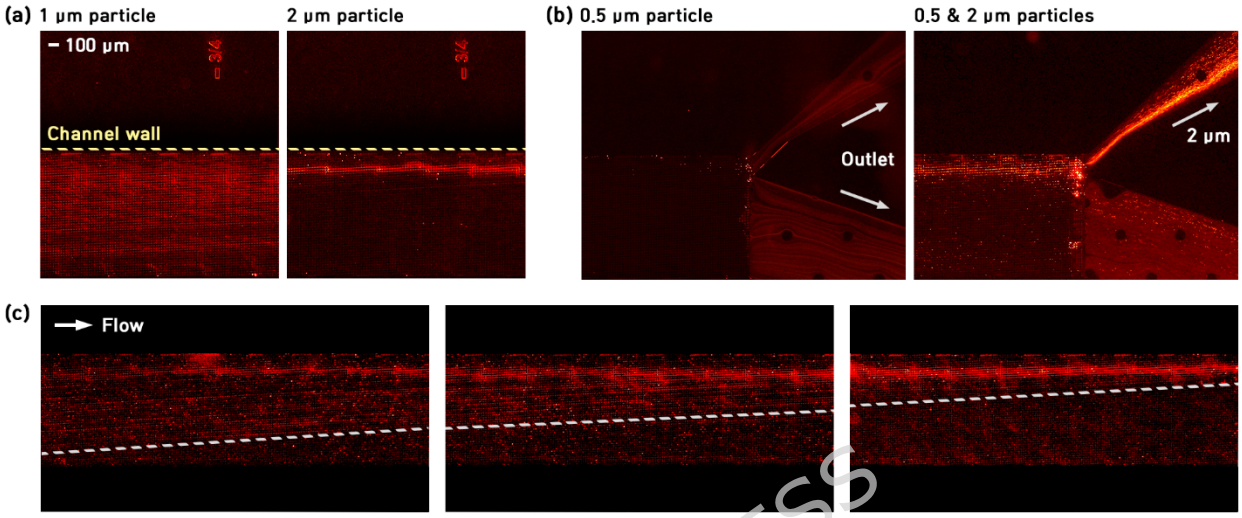

Figure 6 Trajectories of fluorescent particles inside a micropillar array: (a) Comparison of flow images for 1-µm and 2-µm particles at the same position in the array, (b) Flow patterns of 0.5-µm particles alone versus a mixed sample of 0.5-µm and 2-µm particles at the outlet, (c) Flow images of 2-µm particles at different positions from upstream to downstream, showing progressive lateral displacement.

3.2. Nanoemulsion Separation

To quantify the separation performance of the DLD channel, separation experiments were conducted with two different oil emulsion samples. The first oil sample, shown in **Figure 7a**, had a mean diameter of 1.1 µm with a distribution from 669 nm to 1.59 µm. The sample was injected at a flow rate of 2 mL/h. To quantitatively assess this, samples (1 mL each) were collected from the outlets of three identical chips, and their particle size distributions were analyzed. The results (Case 1–3) show nearly identical size distributions, demonstrating high

reproducibility. The median diameter (D_{50}) of the control sample was 1.103 μm, while the median diameter of the separated samples was 0.768 μm, confirming the removal of larger particles. The cumulative distribution graph on the right shows that not only the D_{50} value but also the D_{90} value (representing the 90th percentile) decreased, indicating a significant reduction in the larger droplet population.

Figure 7b shows the separation results for a different oil sample with a mean diameter of 1.1 μm but a broader initial distribution from 660 nm to 2.31 μm. Compared to the previous sample, this control sample contained a larger fraction of coarse droplets. After separation, a significant reduction in particles larger than 1 μm was again observed. The median diameters for the control and separated samples were 1.120 μm and 0.731 μm, respectively, which is similar to the previous result. This indicates that the PDMS chip, based on a consistent DLD array design, can produce samples with a similar final median particle size even when processing emulsions with different initial distributions.

Stability evaluation was performed using a sample with the average diameter (~ 0.7 μm) as the sample with the post-processing device applied (**Supplement Figure 1**). Transmission and backscattering signal changes were analyzed using a Turbiscan device at 6-hour intervals over a 7-day period under room temperature conditions. No significant changes were observed in either signal, indicating that the emulsion maintained dynamic stability without noticeable phase separation for at least 7 days. The phase separation behavior is not solely governed by the Laplace pressure, and it is significantly influenced by the relative magnitude of forces such as gravity and Brownian motion[11]. When particle sizes are smaller than the threshold diameter, Brownian motion dominates the system, reducing the rate of phase separation [11]. This is because the smaller droplets exhibit greater thermal motion,

which counters the effect of gravity and delays the coalescence process. In this study, the post-processing procedure reduces the droplet size to this range, where Brownian motion becomes a dominant factor. As a result, the spatial dispersion of the droplets is maintained.

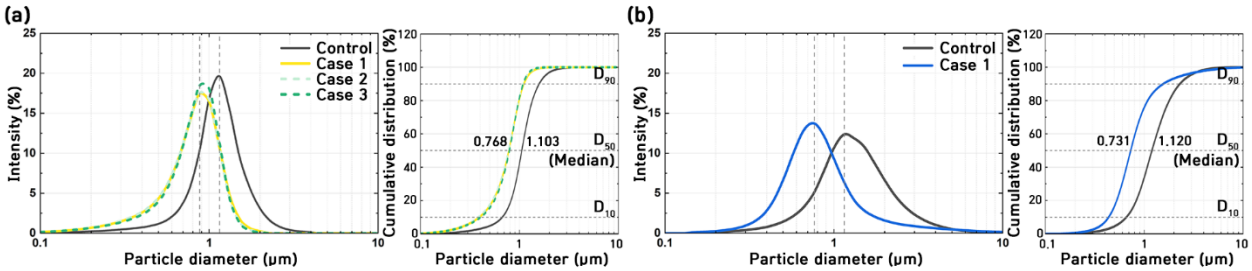

Figure 7. Particle size distribution of nanoemulsion samples before and after DLD separation. (a) Results for a sample with a relatively narrow initial size distribution, showing high reproducibility across three different chips (Case 1-3). (b) Results for a sample with a broader initial size distribution. Both frequency and cumulative distribution curves are shown.

4. Discussion

The oil emulsion separation experiments using our fabricated DLD chip demonstrated particle separation consistent with theoretical principles, effectively achieving separation at the sub-micron level. While conventional microfluidic DLD chips typically employ pillar gaps in the range of tens of micrometers, the device was specifically designed with a significantly narrower gap of 5 μm, to reduce the theoretical critical diameter. This design choice allowed us to selectively remove the larger fraction of oil droplets, successfully shifting the median particle diameter (D_{50}) of the emulsion into the sub-micron range.

Despite these results, there are several limitations to overcome for the separation of even smaller particles and for practical applications. The critical diameter is determined by the pillar gap and array structure, and achieving a smaller D_c requires narrowing the pillar gap. However, excessively narrow gaps increase the risk of structural deformation or damage during the SU-8 master mold fabrication and PDMS replication processes. Furthermore, to increase throughput within a fixed channel width, the channel height must be increased. The SU-8 photolithography and PDMS molding process used in this study has technical limitations in creating high-aspect-ratio structures. Utilizing fabrication methods better suited for high-aspect-ratio structures could help achieve both a smaller D_c and higher throughput simultaneously.

Additionally, the micropillar array introduces significant hydraulic resistance, requiring high pressure to achieve high throughput. PDMS chips, due to the material properties and bonding methods, cannot withstand high fluid pressures. Increasing the flow rate can cause leakage at the chip-to-substrate or tube-to-chip interfaces, or even channel deformation, which degrades separation performance. Consequently, stable separation was only possible at a low flow rate of 2 mL/hr in the current PDMS-based device.

Future work should focus on fabricating high-aspect-ratio microfluidic chips using more rigid materials to overcome these limitations by the pressure tolerance of the material. For example, fabricating devices from materials like glass or rigid polymers could enable the creation of robust, high-aspect-ratio structures capable of stable operation at high flow rates. Furthermore, expanding the design from the current two parallel channels to a massive multi-channel array will facilitate the high-throughput processing required for industrial-scale applications.

5. Conclusions

In this study, we successfully designed, fabricated, and tested a DLD microfluidic chip for the passive separation of large oil droplets from an O/W nanoemulsion. The device, with a critical diameter of approximately 1.7 μm, effectively removed larger droplets, resulting in a significant reduction in the median particle size and a more homogeneous emulsion. The experimental results, supported by numerical simulations and fluorescent bead tracking, validate the DLD approach as a viable post-processing step for improving emulsion quality and stability. While the current PDMS-based platform has throughput limitations, this study demonstrates the potential of DLD technology and lays the groundwork for future development using more robust materials for high-throughput industrial applications. For the future work, the channels designed in this study will be fabricated with various materials to ensure consistency in manufacturing. At the same time, robust materials will be selected to maintain the verticality of the micro pillars, and optimization will be carried out to enable operation under higher pressure conditions. Through this, a module including the microfluidic chip will be created and connected in parallel, ultimately leading to the development of a device that can operate at higher flow rates.

Acknowledgments

This work was supported by the Fostering Program for the R&D Industry Promotion Complex (2710019690), the Research Initiative Program (CRC22023-000), and the National Research Council of Science & Technology (NST) grant (No. GTL24022-000), funded by the Korea government (MSIT)

Funding

This work was supported by the Fostering Program for the R&D Industry Promotion Complex (2710019690), the Research Initiative Program (CRC22023-000), and the National Research Council of Science & Technology (NST) grant (No. GTL24022-000), funded by the Korea government (MSIT)

Data availability

The datasets used and/or analysed during the current study available from the corresponding author on reasonable request.

References

1. Ozogul, Y. *et al.* Recent developments in industrial applications of nanoemulsions. *Adv. Colloid Interface Sci.* **304**, 102685 (2022).
2. Aziz, Z. A. A. *et al.* Role of Nanotechnology for Design and Development of Cosmeceutical: Application in Makeup and Skin Care. *Front. Chem.* **Volume 7-2019**, (2019).
3. Yousefpoor, Y., Esnaashari, S. S., Baharifar, H., Mehrabi, M. & Amani, A. Current challenges ahead in preparation, characterization, and pharmaceutical applications of nanoemulsions. *WIREs Nanomedicine Nanobiotechnology* **15**, e1920 (2023).
4. McClements, D. J. & Rao, J. Food-grade nanoemulsions: formulation, fabrication, properties, performance, biological fate, and potential toxicity. *Crit. Rev. Food Sci. Nutr.* **51**, 285–330 (2011).
5. Schultz, S., Wagner, G., Urban, K. & Ulrich, J. High-pressure homogenization as a process for emulsion formation. *Chem. Eng. Technol. Ind. Chem. Equipment-Process Eng.* **27**, 361–368 (2004).

6. Canselier, J., Delmas, H., Wilhelm, A. & Abismail, B. Ultrasound emulsification—an overview. *J. Dispers. Sci. Technol.* **23**, 333–349 (2002).
7. Mathews, H. F., Pieper, M. I., Jung, S. & Pich, A. Compartmentalized Polyampholyte Microgels by Depletion Flocculation and Coacervation of Nanogels in Emulsion Droplets. *Angew. Chem. Int. Ed.* **62**, e202304908 (2023).
8. Geng, Y. & Yu, J. Progress in constructing functional coacervate systems using microfluidics. *BMEMat* **2**, e12058 (2024).
9. Liu, X. *et al.* Stability Characteristics of Dispersed Oil Droplets Prepared by the Microchannel Emulsification Method. *J. Colloid Interface Sci.* **233**, 23–30 (2001).
10. Yeh, S.-L., Koshani, R. & Sheikhi, A. Colloidal aspects of calcium carbonate scaling in water-in-oil emulsions: A fundamental study using droplet-based microfluidics. *J. Colloid Interface Sci.* **633**, 536–545 (2023).
11. Hwangbo, S.-A., Lee, S.-Y., Kim, B.-A. & Moon, C.-K. Preparation of Surfactant-Free Nano Oil Particles in Water Using Ultrasonic System and the Mechanism of Emulsion Stability. *Nanomaterials* **12**, (2022).
12. Jin, W. *et al.* 1 - Nanoemulsions for food: properties, production, characterization, and applications. in *Emulsions* (ed. Grumezescu, A. M.) 1–36 (Academic Press, 2016). doi:10.1016/B978-0-12-804306-6.00001-5.
13. Gehrmann, S. & Bunjes, H. Influence of membrane material on the production of colloidal emulsions by premix membrane emulsification. *Innov. Process. Bio-Pharm. Poorly Water-Soluble API* **126**, 140–148 (2018).
14. Liu, M., Li, J. & Guo, Z. Polyaniline coated membranes for effective separation of oil-in-water emulsions. *J. Colloid Interface Sci.* **467**, 261–270 (2016).
15. Li, P. *et al.* Density gradient ultracentrifugation for colloidal nanostructures separation and investigation. *Sci. Bull.* **63**, 645–662 (2018).
16. Bayareh, M. An updated review on particle separation in passive microfluidic devices. *Chem. Eng. Process. - Process Intensif.* **153**, 107984 (2020).
17. Song, Y., Li, D. & Xuan, X. Recent advances in multimode microfluidic separation of

particles and cells. *ELECTROPHORESIS* **44**, 910–937 (2023).

18. Huang, L. R., Cox, E. C., Austin, R. H. & Sturm, J. C. Continuous Particle Separation Through Deterministic Lateral Displacement. *Science* **304**, 987–990 (2004).
19. Tottori, N., Hatsuzawa, T. & Nisisako, T. Separation of main and satellite droplets in a deterministic lateral displacement microfluidic device. *RSC Adv.* **7**, 35516–35524 (2017).
20. Holmes, D. *et al.* Separation of blood cells with differing deformability using deterministic lateral displacement†. *Interface Focus* **4**, 20140011 (2014).
21. Liu, Z. *et al.* Integrated Microfluidic Chip for Efficient Isolation and Deformability Analysis of Circulating Tumor Cells. *Adv. Biosyst.* **2**, 1800200 (2018).
22. Xavier, M. *et al.* Label-free enrichment of primary human skeletal progenitor cells using deterministic lateral displacement. *Lab. Chip* **19**, 513–523 (2019).
23. Chen, Y. *et al.* Concentrating Genomic Length DNA in a Microfabricated Array. *Phys. Rev. Lett.* **114**, 198303 (2015).
24. Wunsch, B. H. *et al.* Nanoscale lateral displacement arrays for the separation of exosomes and colloids down to 20 nm. *Nat. Nanotechnol.* **11**, 936–940 (2016).
25. Kim, S.-C. *et al.* Broken flow symmetry explains the dynamics of small particles in deterministic lateral displacement arrays. *Proc. Natl. Acad. Sci.* **114**, E5034–E5041 (2017).
26. McGrath, J., Jimenez, M. & Bridle, H. Deterministic lateral displacement for particle separation: a review. *Lab. Chip* **14**, 4139–4158 (2014).
27. Zeming, K. K., Salafi, T., Chen, C.-H. & Zhang, Y. Asymmetrical Deterministic Lateral Displacement Gaps for Dual Functions of Enhanced Separation and Throughput of Red Blood Cells. *Sci. Rep.* **6**, 22934 (2016).
28. Davis, J. A. Microfluidic Separation of Blood Components through Deterministic Lateral Displacement. in (2008).
29. Davis, J. A. *et al.* Deterministic hydrodynamics: Taking blood apart. *Proc. Natl. Acad. Sci.* **103**, 14779–14784 (2006).